Constraining the Spatial Distribution of Tritium in Groundwater across South Africa

Jared David van Rooyen[1], Jodie Miller[2], Andrew Paul Watson[1], and Laszlo Palcsu[3]

[1]Stellenbosch University
[2]University of Stellenbosch Faculty of Science
[3]Isotope Climatology and Environmental Research Centre, Institute for Nuclear Research

November 23, 2022

Abstract

Tritium (^{3}H) has become synonymous with modern groundwater and is used in a myriad of applications, ranging from sustainability investigations to contaminant transport and groundwater vulnerability. This study uses measured ^{3}H groundwater activities from 722 samples locations across South Africa to construct a ^{3}H groundwater distribution surface. Environmental co-variables are tested using geostatistical analysis to constrain external controls on ^{3}H variability, namely: [1] depth to the water table, [2] distance from the ocean and [3] summer vs winter rainfall proportion. The inclusion of co-variables in the 'fit' of residual variograms improved prediction variance significantly, yet does not mitigate issues with sample density. The distribution of ^{3}H in groundwater surface agrees well to expected controls, with proximal (<100km) coastal regions, winter rainfall zones and deeper groundwater tables predicted to have lower ^{3}H activities. Conversely, inland localities with shallower water tables and/or summer rainfall are predicted to have elevated ^{3}H activities. High groundwater ^{3}H anomalies could potentially be attributed to uranium-bearing deposits, as geogenic production of ^{3}H amplifies the activity contributed through recharge. Some ^{3}H high and low anomalies cannot be explained by known phenomena and may simply be regions of variable recharge and/or longer isolated groundwater flow paths. Regions of active recharge are more vulnerable to climate change as well as modern pollution. Less actively recharged groundwater may be more resilient to climate change, yet represents a potentially non-renewable resource for abstraction. The application of ^{3}H distributions in the assessment of hydrological resilience is pertinent to effective groundwater management studies.

Constraining the Spatial Distribution of Tritium in Groundwater across South Africa

J.D. van Rooyen[1], A.P. Watson[1], L. Palcsu[2] and J.A. Miller[1]

[1]Department of Earth Sciences, Faculty of Sciences, University of Stellenbosch, Private Bag X1, Matieland, 7601, South Africa. jvanrooyen121@gmail.com, 15661547@sun.ac.za, jmiller@sun.ac.za.

[2]Isotope Climatology and Environmental Research Centre (ICER), Institute for Nuclear Research, H-4026 Debrecen, Bem tér 18/c, Hungary. palcsu@atomki.mta.hu

Corresponding author: Jared van Rooyen (jvanrooyen121@gmail.com)

Key Points:

- 722 groundwater ^3H samples across South Africa
- Geostatistical analysis of the 3 co-variables in ^3H spatial structure
- Lower ^3H activity with depth, coastal proximity and winter rainfall region
- Higher ^3H activity with inland localities, summer rainfall regions and U deposits
- Implications for sustainable groundwater management and hydrological resilience

Abstract

Tritium (^3H) has become synonymous with modern groundwater and is used in a myriad of applications, ranging from sustainability investigations to contaminant transport and groundwater vulnerability. This study uses measured ^3H groundwater activities from 722 samples locations across South Africa to construct a ^3H groundwater distribution surface. Environmental co-variables are tested using geostatistical analysis to constrain external controls on ^3H variability, namely: [1] depth to the water table, [2] distance from the ocean and [3] summer vs winter rainfall proportion. The inclusion of co-variables in the 'fit' of residual variograms improved prediction variance significantly, yet does not mitigate issues with sample density. The distribution of ^3H in groundwater surface agrees well to expected controls, with proximal (<100km) coastal regions, winter rainfall zones and deeper groundwater tables predicted to have lower ^3H activities. Conversely, inland localities with shallower water tables and/or summer rainfall are predicted to have elevated ^3H activities. High groundwater ^3H anomalies could potentially be attributed to uranium-bearing deposits, as geogenic production of ^3H amplifies the activity contributed through recharge. Some ^3H high and low anomalies cannot be explained by known phenomena and may simply be regions of variable recharge and/or longer isolated groundwater flow paths. Regions of active recharge are more vulnerable to climate change as well as modern pollution. Less actively recharged groundwater may be more resilient to climate change, yet represents a potentially non-renewable resource for abstraction. The application of ^3H distributions in the assessment of hydrological resilience is pertinent to effective groundwater management studies.

Plain Language Summary

Scientists, who try understand the water cycle, use isotopes to track how water moves from rain to rivers and groundwater. In this study, we use one isotope called tritium, which is a heavy and unstable form of hydrogen (^3H), to identify rain water that has reached groundwater in modern times (50-100 years). Modern groundwater is not only a renewable resource, but it is also vulnerable to climate change and modern pollution. We collected 722 tritium samples and used a model to predict how much tritium is in groundwater across the country of South Africa. The model found that coastal areas, that receive winter rainfall and/or have deeper groundwater generally have less tritium than inland, summer rainfall and/or shallow groundwater areas. This is partially explained by the amount of tritium in the rain that these regions receive or the time it takes for the rain to get to the groundwater. The central Karoo region and north eastern regions of South Africa had the most actively recharged groundwater and that the west coast and northern Karoo had the least. Understanding how much water reaches groundwater helps scientists advise policy makers, who create strategies to use water sustainably and protect it from pollution.

1 Introduction

Groundwater represents the most abundant freshwater resource available to both humans and the environment (Gleeson et al., 2015), especially in semi-arid to arid regions where surface water is scarce (Schoups et al., 2005). Use of groundwater is rapidly increasing as a result of climate change as well as the need for increased food production due to population growth (Cuthbert et al., 2019; Díaz-Cruz and Barceló, 2008; Ferguson and Gleeson, 2012; Gleeson et al., 2015; Zhang et al., 2001). As a result, groundwater is becoming progressively more vulnerable to depletion and contamination (van Rooyen et al., 2020b; Villholth et al., 2013; Wada et al., 2010). As groundwater dependence increases, so does the need to understand a catchments ability to absorb disturbance and maintain or quickly regain hydrologic function, known as a catchment's hydrological resilience (Mao et al., 2017). Additionally, modern recharge mechanisms, which control a catchments hydrological resilience, are changing due to climate change, land use change and shifts in resource utilization (Meixner et al., 2016). In order to quantify the hydrological resilience of a catchment, a comprehensive understanding of the catchments hydrological structure, water balance, cyclical climate fluctuations and anthropogenic influence is typically needed. Yet, alternative methods that use environmental isotopes can provide an understanding of proportions of modern recharge and enable an early assessment of hydrological resilience without an abundance of data.

Progress in the field of spatial isotope statistics has validated the use of environmental isotopes in a myriad of applications (West et al., 2009). Conservative tracers (e.g. stable isotopes) of the hydrological cycle can determine spatial variations in recharge rates and zones (Vengosh et al., 2002), water-rock interaction (Gillon et al., 2009), pollution potential (Hagedorn et al., 2018), aquifer connectivity and salinization processes (Bennetts et al., 2006). Although less common, non-conservative (e.g. radioactive isotopes) tracers have also been successfully used in spatial models to predict groundwater age distributions (Visser et al., 2016). Tritium (^{3}H), which has a half-life of 12.312 years (Lucas and Unterweger, 2000; MacMahon, 2006), has become synonymous with modern groundwater or groundwater that has been recharged within the last ~50-100 years (Hagedorn et al., 2018; Jasechko et al., 2017; Le Gal La Salle et al., 2001; Li et al., 2019; Palcsu et al., 2017; Samborska et al., 2013; Visser et al., 2016; Zuber et al., 2005). The popularity of methods that use ^{3}H was invigorated by the increase in atmospheric abundance of ^{3}H through thermonuclear bomb testing in the 1950s and 1960s (Schlosser et al., 1989). Subsequently, the attenuation of 'bomb' ^{3}H has resulted in modern precipitation only incorporating natural levels of ^{3}H, particularly in the southern hemisphere where the bomb peak was much lower (Stewart, 2012). As ^{3}H forms part of the water molecule, its behavior in recharge is chemically conservative and radioactive decay is the predominant process controlling its abundance along a groundwater flow path. The assessment of natural levels of ^{3}H in recharge presents new challenges and opportunities in the prediction of the proportion and spatial distribution of modern groundwater (Morgenstern et al., 2010).

Recent research used ^{3}H data collected over diverse climatic and hydrogeological environments to estimate the global distribution and volume of modern groundwater (Gleeson et al., 2016). Yet, global investigations are less applicable at catchment scale, where seasonal fluctuation, land use change and shifts in resource use can disrupt the hydrological cycle. It is also evident that the variation of background ^{3}H in local rainfall is more significant than reported in older studies (Kern et al., 2020; van Rooyen et al., 2020a; Visser et al., 2018). Once ^{3}H reaches the subsurface through recharge, its abundance is predominantly dependent on decay as the subsurface production of ^{3}H is limited to areas nearby radioactive deposits, landfills or waste sites (Hughes et al., 2011). If an aquifer system does not contain detectable levels of ^{3}H, it is either no longer being actively recharged and/or the isolated flow path is long enough to allow for ^{3}H to decay below detection limits. The ability of ^{3}H to distinguish between modern and older groundwater provides insight to how resilient an aquifer may be to disruptions in the hydrological cycle. Furthermore, evaluation of the distribution of modern groundwater via the use of ^{3}H is applicable for regions where physical groundwater monitoring is intermittent, inconsistent and/or sparse.

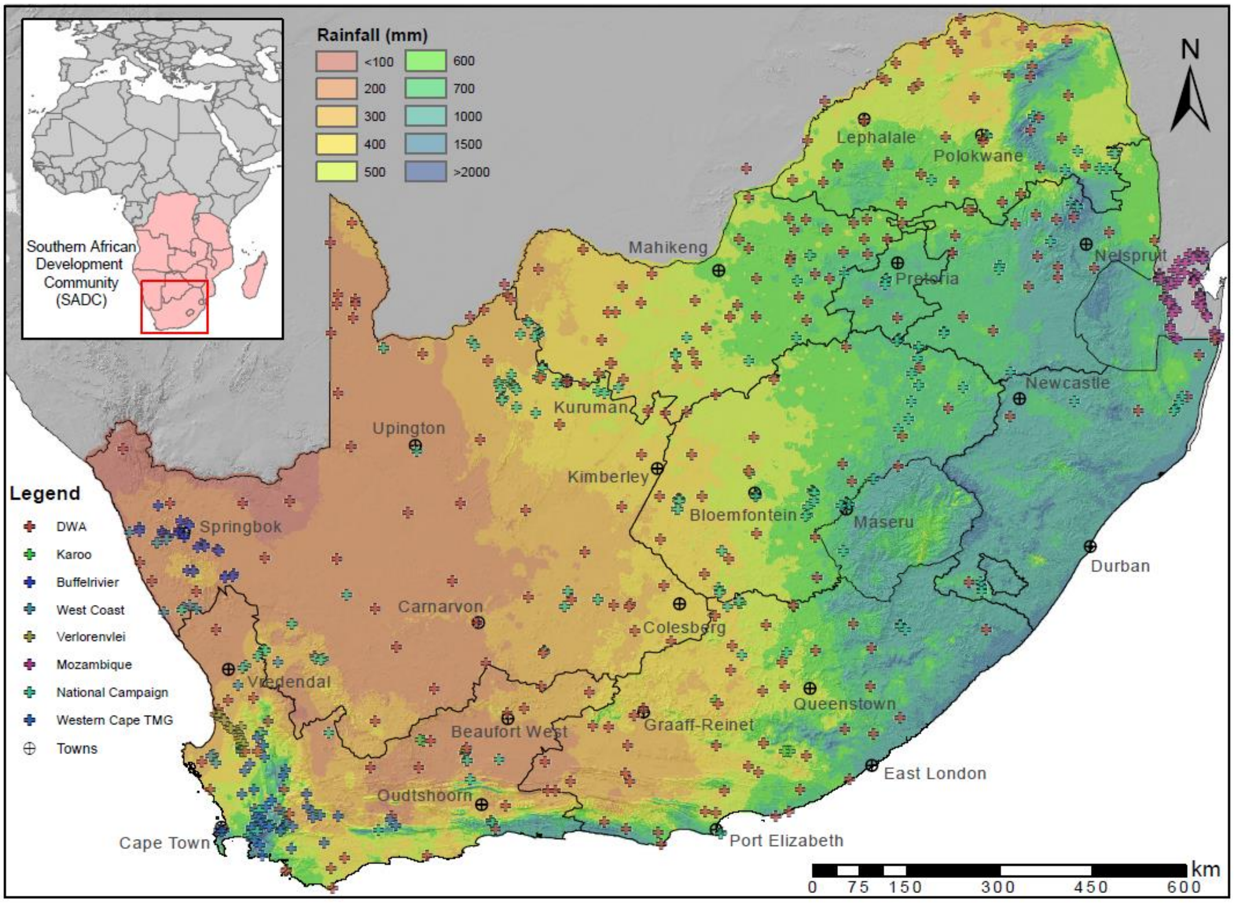

Figure 1 - The distribution of ^{3}H in groundwater sample locations as well as the major towns in South Africa. Mean annual precipitation is represented in mm in ten classes (Schulze et al., 2006).

South Africa is a large country (1.22 million km^2) with a diverse climate that ranges from semi-arid to arid in the central and western reaches to sub-tropical on the east coast and temperate in the north-east. Rainfall seasonality is divided across the country into semi-distinct summer and winter rainfall regions (Roffe et al., 2019) (Fig.1). Mean annual rainfall ranges from <100 mm in the arid Northern Cape Province to a peak of 3500 mm in the high altitude eastern interior (Schulze et al., 2006) (Fig.1). As a consequence South Africa, by global standards, is a water scarce country and the agricultural industry as well as an increasing populace is dependent on sustained groundwater availability. Yet, a significant portion of the country's geology, is represented by large hard rock provinces that lack major groundwater aquifers (Basson et al., 1997). The largest aquifer system in South Africa is within the Karoo Basin and provides significant amounts of fresh water to an otherwise semi-arid region. Smaller aquifer systems occur in the Cape Fold Belt as well as in carbonate terrains of Limpopo and North West Provinces. Additionally, South Africa shares three major transboundary aquifer systems, the largest of which is the Stampriet aquifer between Namibia, Botswana and South Africa (Cobbing et al., 2008). Due to the heterogeneous nature of groundwater reservoirs in South Africa and increasing groundwater dependence, constraining the resilience of groundwater is important for effective groundwater management.

This study investigates the spatial distribution of ^{3}H in groundwater in South Africa through the statistical assessment of: [1] measured ^{3}H in groundwater (n=722), [2] local variability of ^{3}H in rainfall and [3] the impact of unsaturated zone travel time during recharge on ^{3}H activity. To assess the effect of ocean dilution and rainfall seasonality, localities of groundwater samples are grouped into regions where the activity of ^{3}H in recharge is expected to differ as a result of atmospheric processes. To estimate the effect of unsaturated zone travel time, water table data are collated from South Africa's National Groundwater Archive (NGA) and modelled into a predictive static water level surface. Environmental co-variables are used to constrain external drift in predictions of ^{3}H in groundwater, with the "drift" being the value of the co-variable identified to explain a portion of variance within the testing parameter, in this case ^{3}H. As temporal climate records are insufficient across most of Africa to assess climate change over the past century, tracers of the hydrological cycle contribute invaluable information to policy makers (Niang et al., 2014). Understanding modern groundwater recharge is pertinent to assessing the effects of climate change on water resources, as well as groundwater mixing relationships and vulnerability estimates to both depletion and contamination.

2 Materials and Methods

This study collected groundwater samples across South Africa in a series of sampling campaigns for the purpose of constraining the distribution of ^{3}H activity in groundwater. To improve the sample size and spatial distribution of samples used for interpolation, data from previous studies was incorporated into the dataset. Co-variables to ^{3}H data were determined from environmental data to remove any spatial structure that is dependent on factors other than the subsurface decay of ^{3}H. Following this approach, a ^{3}H distribution surface for South Africa was created using a Kriging with External Drift (KED) method and interpreted in the environmental context of South Africa.

2.1 Sampling strategy

Groundwater samples were collected during seven sampling campaigns across South Africa. These campaigns resulted in the collection of 446 samples (Fig.1). Sample groups were formed according to the sampling campaigns used to collect groundwater samples as follows: [1] west coast of South Africa (n=23), [2] Verlorenvlei RAMSAR protected catchment (n=19), [3] Buffelsriver watershed (n=32), [4] Karoo basin (n=20), [5] Western Cape Table Mountain Group (n=59), [6] southern Mozambique (n=95) and, [7] 'Know Your Water' citizen science sampling campaign (n=198). Samples analysed for ^{3}H were collected in 1 liter polypropylene high density amber sampling bottles, completely filled to avoid atmospheric contamination. Additionally, all pumped well points were sufficiently purged to ensure the groundwater sample was representative of the contributing aquifer. Detailed records of casing depths, screen lengths/depths and well depths were not always available, especially for older well points, the implications of which are explored in the discussion. Additional samples (n=276) (Fig.1) were collated from a database of samples analysed by iThemba Labs (WITS), Johannesburg as well as a database provided by the South African Department of Water Affairs (DWA). All iThemba Labs samples were collected and analysed in 2006 and are available online as supplementary Table A.I.

2.2 Analysis

Groundwater samples collected from 2017-2019 were sent for analysis at the Isotope Climatology and Environmental Research Centre (ICER), Institute for Nuclear Research in Debrecen, Hungary. Analysis of ^3H at ICER was done using the ^3He ingrowth method (Palcsu et al., 2010; Papp et al., 2012). This analysis involves degassing the water sample and measuring the newly produced ^3He gas from ^3H decay using a dual collector (noble gas) mass spectrometer, after a predetermined length of time. The method has a detection limit of 0.012 TU and expectation values are within 2 % for samples between 1 and 20 TU. ^3H measurement included in this study that were collated from other South African studies were analysed at iThemba labs (WITS) in Johannesburg, South Africa, using the liquid scintillation counter (LSC) and electrolytic enrichment method (Plastino et al., 2007). The method has a detection limit of 0.1 TU. Data included from other studies carries inherent uncertainties associated with spatial delineations and interpolated values, but this uncertainty is not constrained in the context of this study.

2.3 Measured ^3H in groundwater

Groundwater ^3H activities measured as part of this study had a mean ^3H activity of 0.64 TU (n=446) and a range of 0 – 3.5 TU. The standard deviation of the sample dataset was 0.63. Samples collected on the west coast sampling campaign had a mean ^3H activity of 0.68 TU and a range of 0 – 1.4 TU (σ = 0.49). Samples collected in the Verlorenvlei watershed had a mean ^3H activity of 0.19 TU and a range of 0 – 0.62 TU (σ = 0.17). Samples collected the Buffelsriver watershed are had a mean ^3H activity of 0.41 TU and a range of 0 – 1.58 TU (σ = 0.40). Samples collected in the central Karoo had a mean ^3H activity of 0.92 TU and a range of 0 – 3.50 TU (σ = 0.93). Samples collected in the Western Cape sampling campaign had a mean ^3H activity of 0.73 TU and a range of 0 – 3.22 TU (σ = 0.59). Samples collected from the ‘Know Your Water’ citizen science sampling campaign had a mean ^3H activity of 0.82 TU and a range of 0 – 3.4 TU (σ = 0.67). Samples collected in southern Mozambique had a mean ^3H activity of 0.28 TU and a range of 0 – 2.04 TU (σ = 0.36). Samples collated from previous studies are well distributed across South Africa and had a mean ^3H activity of 1.26 TU and a range of 0 – 4.8 TU (σ = 1.02). The modal statistics are summarized in Figure 2. Measured groundwater ^3H activities summarized above are available online as supplementary Table A.II.

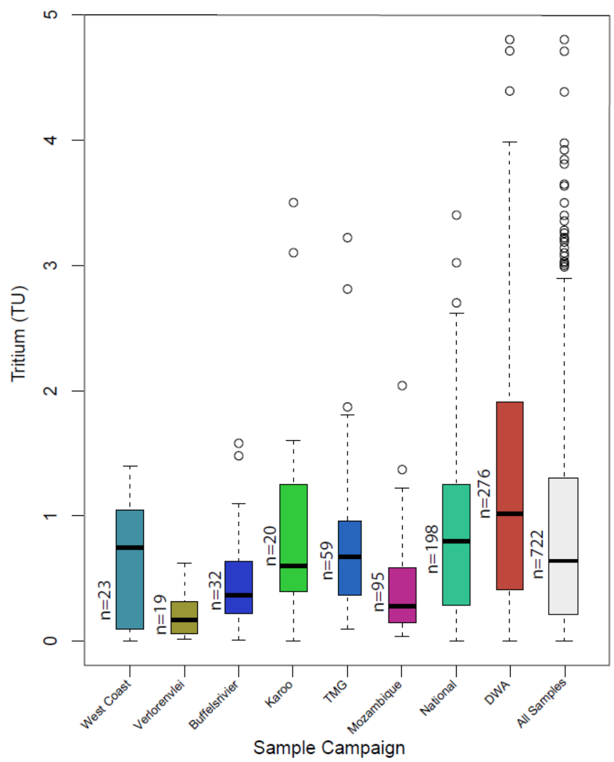

Figure 2 - Box plot showing the basic ^{3}H model statistics of the seven sampling campaigns used to collect groundwater in this study as well as the DWA database used to supplement the collected groundwater data.

2.4 Environmental co-variables

The co-variables investigated in this study were included from known controls on the activity of ^{3}H in groundwater (Harms et al., 2016; Visser et al., 2016). The co-variables used to assess external drift were identified as: [1] depth to the water table, [2] distance from the ocean and [3] summer vs winter rainfall proportion. As the travel time of recharge in the unsaturated zone may result in significant decay of ^{3}H before it reaches the water table, it is important to remove this potential control, before identifying the spatial structure of ^{3}H variability in groundwater. Although many collected samples have associated water level measurements taken during sample collection, these measurements are often not representative of the static water levels in the region or the aquifer. To mitigate assumptions made from spot sampling groundwater levels, a large national database (DWAF, 2004) (n=126531) of static water levels was used to interpolate a 'depth to groundwater' surface that predicted the static water level for the sample locations. This surface was produced using the same ordinary kriging methodology as other geo-spatial statistics in this study.

The background activity of ^{3}H in precipitation is largely controlled by the origin of the water mass that produces local precipitation (van Rooyen et al., 2020a; Visser et al., 2018). A HYSPLIT model, which calculates air mass trajectories, can be used to predict water mass origin and in turn, the likely effect on local ^{3}H activity in precipitation. Regions that haved receive rainfall predominantly in different times of the year, will be affected by intra-annual variability of ^{3}H due to seasonality. Summer vs winter rainfall zones are delineated into eight categories according to the combined agreement of previous delineations of winter summer rainfall zones (Roffe et al., 2019). Furthermore, coastal rainfall generally has lower ^{3}H activities due the effect of ocean water dilution (van Rooyen et al., 2020a). The Euclidean distance to the ocean was calculated in ArcGIS to produce a 10x10 km grid to assess the control of ocean dilution.

2.5 Data Preprocessing

To assess the degree of local spatial dependence of ^{3}H in groundwater, where samples collected closer in geographical space imply similar ^{3}H activities, the spatial autocorrelation of the dataset must be determined. This can be expressed as the strength of correlation depending on separation distance, where the correlation is expressed as the semivariance. Each pair of observations has an associated semivariance (γ) defined as:

$$\gamma(x_i, x_j) = \frac{1}{2}[z(x_i) - z(x_j)]^2 \quad (1)$$

where x is a specific geographical point and $z(x)$ is the associated attribute value, in this case ^{3}H in TU. A variogram cloud outlier detection procedure (Ploner, 1999) was applied to the collated ^{3}H database used in this study. The variogram cloud function reports the semivariance of point pairs within a particular neighborhood radius. The resultant pairs that deviate significantly from nearby observations, exceeding a semivariance of γ=1, were further investigated to constrain whether there could be a possible analytical error or if one sample was collected from a deeper confined aquifer system. To avoid samples being coupled with samples that were collected in a vastly different environment (subtropical vs semi-arid, coastal vs inland), the search neighborhood was limited to the highest average variogram range (~200km). Four sample point pairs were identified using this method and two of the eight investigated samples were removed as their measurement uncertainty was too high (>0.8 TU) (Fig.3).

The pairwise semivariances were then calculated for each sample location within the ~200km search radius to group samples into search neighborhoods. It was found that the standardized mean differences fell predominantly within ±1 interval (88%) and only 12 samples fell outside the ±5 interval range (1.6%). This range was used as the cutoff range for the possibility if erroneous data. The twelve identified samples were further interrogated, yet were determined to be representative samples and thus included in further calculations.

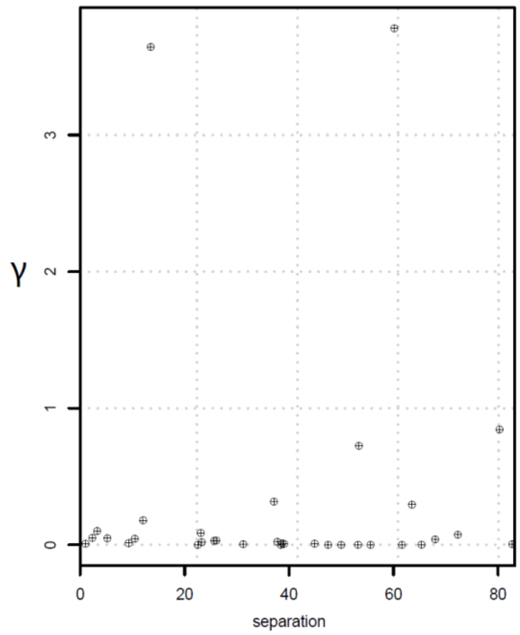

Figure 3 - The semivariance of point pairs computed as a variogram cloud in the data outlier analysis. Semivariance is represented as the average γ for a point pair as calculated in equation 1.

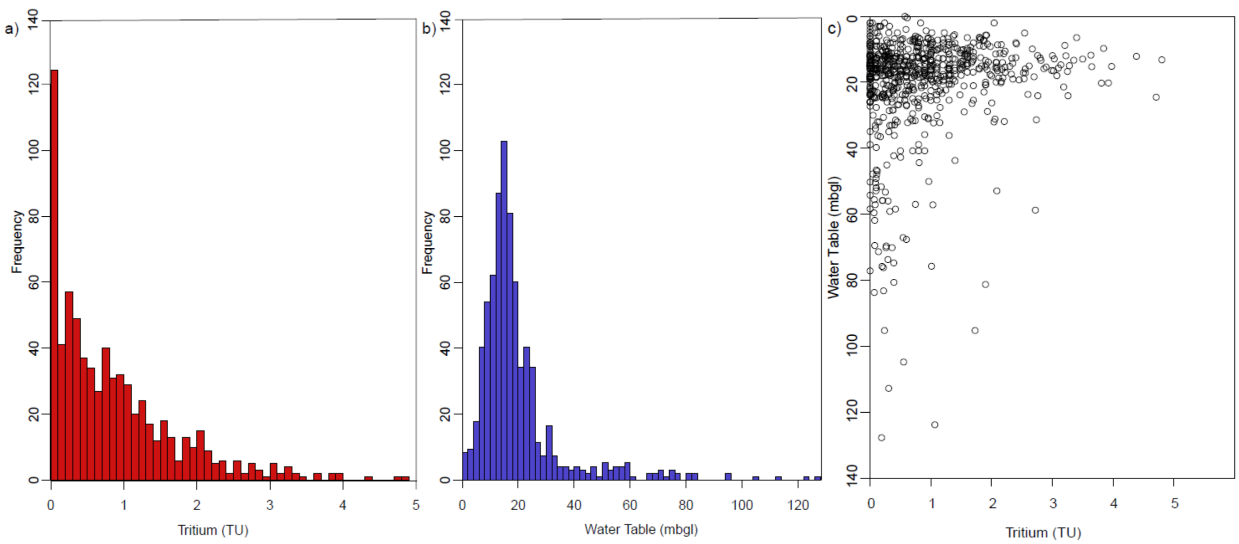

Figure 4 - The frequency distribution of a) measured ^3H (Tritium Units) in groundwater and b) the predicted depth to groundwater table (meters below ground level) of all 722 samples. The relationship of ^3H and depth to groundwater table is plotted in c).

A similar outlier detection technique was applied to the collated groundwater levels database resulting in a small subset of readings excluded from further calculations (0.17%). Previous research, that used global groundwater ^3H records, observed a robust trend in decreasing ^3H with depth to the water table as well as depth below the water table (Gleeson et al., 2016). The groundwater data in this study showed a similar pattern, yet where the water table was shallower there was a significant variation in ^3H values (Fig.4). The heterogeneous distribution of hydraulic conductivities in shallow aquifers in South Africa and significant variation in recharge ^{3}H activity are likely causes for the variation in shallower boreholes and suggest that the depth to the water table is not the only contributing factor to regional ^{3}H variability. These findings in the pre-processing analysis of data affirmed the inclusion for other atmospheric controls on ^{3}H variability to be included in interpolation techniques.

2.6 Derivation of ^{3}H distribution surfaces

In order to relate the semivariances calculated in preprocessing, to the separation distance calculated from sample locality, an empirical variogram is used. The concept of displaying semivariances according to the separation distance was first proposed and calculated using the Matheron algorithm (Matheron, 1965). The empirical variogram, described as the average separation within some separation range, can be defined as:

$$\bar{\gamma}(h) = \frac{1}{2m(h)} \sum_{(i,j)|h_{ij} \in h} \left[z(x_i) - z\left(x_j\right)\right]^2 \tag{2}$$

where i, j represent the numbered point pair for which the semivariance is computed and h_{ij} is the separation distance between points i and j, h is the range of separations as defined by the histogram bins and $m(h)$ is the number of point-pairs in the bin corresponding to h. As is evident from the preprocessing procedure, some variation in ^{3}H in groundwater can be explained by the environmental co-variable. In order to remove variation attributed to the co-variable, variograms (Chilès, 2012) are constructed from the residual data, as described in Rossiter and Eda, (2019). A residual variogram is computed the same as an empirical variogram, where γ(h) is the semivariogram, and Z(x) and Z(x+h) are the values of a parameter sampled at a planar distance |h| from each other:

$$\bar{\gamma}(h) = \frac{1}{2N(h)} \sum_{i=1}^{N(h)} [Z(x_i) - Z(x_i + h)]^2 \tag{3}$$

where N(h) is the number of lag-h differences. This can be represented by the separation distance between two points, i.e. $n\ x\ (n-1)/2$, and n corresponds to the number of sampling locations at distance h. The fit parameters of a calculated variogram are describe as: [1] the nugget, which represents the variance at the given sample location and captures variability that is independent of spatial autocorrelation, [2] the sill, which is the maximum semivariance of the variogram model and is equal to the sum of the nugget and the partial sill, and [3] the range, which corresponds to the distance at which semivariance is no longer increasing and samples no longer display autocorrelation (Chilès, 2012). The fitting of a variogram model was performed by fitting the range and the sill to the given semivariance point-pairs by:

$$\gamma(h) = \begin{cases} c \cdot \left[\frac{2}{3}\frac{h}{a} - \frac{1}{2}\left(\frac{h}{a}\right)^3\right], & h < a \\ c, & h \geq a \end{cases} \tag{4}$$

where a is the range and c is the sill or maximum semivariance. The entire variogram is raised by the nugget variance. The variogram model was fitted to calculated semivariances for discrete lag intervals by the weighted least squares approach. This lag interval ranged from 10-25km depending on the ordinary or universal kriging method adopted.

For the geostatistical modeling of interpolated data (e.g. kriging), theoretical variograms were fitted to estimate an empirical variogram from the sample dataset. This empirical variogram was fit to have a maximum lag distance of 250 km with 11 equal interval bins (lags) in order to distribute equal sample observations per bin. The effective planar range (a_e), which is equal to the distance in which autocorrelation is significant, was computed to be ~214km. Subsequently, residual variograms were prepared for KED, which are computed on a 10x10 km grid. The co-variables included in this study were computed individually with TU to assess any improvement in the average semivariance of the semivariogram and the distribution of prediction variances of the interpolation.

3 Results

The obtained regional gridded ^{3}H activity in groundwater, independent of external drift, was computed from a fitted semivariogram model which had an average semivariance of 0.559 and planar distance of 214km (Fig.5a). The spatial prediction variance had a distribution localized to sample locations, where regions with few samples formed abrupt increases in variance near sample point locations. A notable increase in prediction variance was observed on the east coast of South Africa, where sample density was poor. Regions of elevated ^{3}H activity were localized to south central regions of the Karoo basin as well as the north eastern regions of the country. Many regions showed a random distribution of ^{3}H activity in groundwater, where erratic changes were observed over relatively short distances.

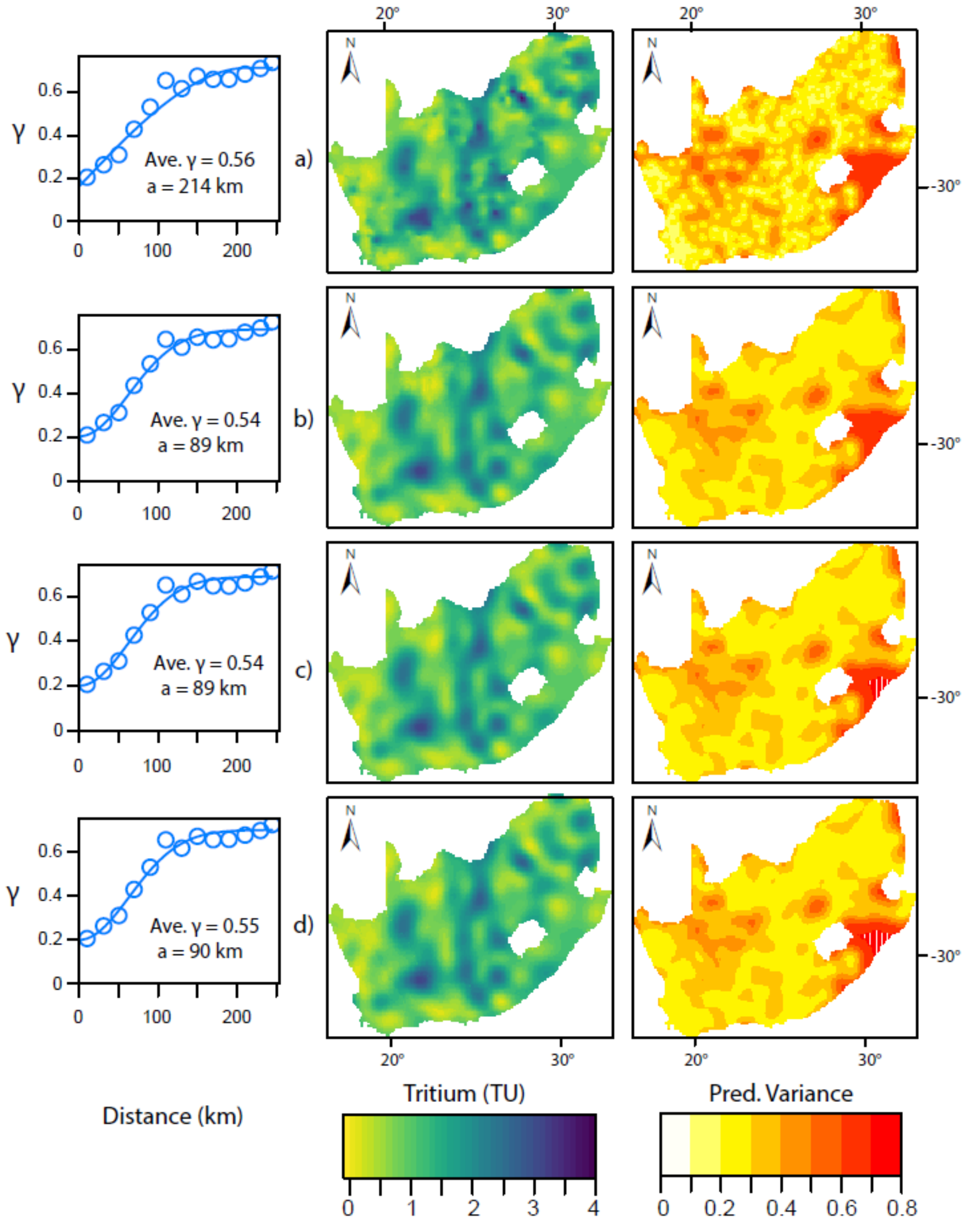

Figure 5 - The geostatistical results for variogram fit, predicted ^3H activity and prediction variance of a) the empirical calculation of ^3H distribution independent on external controls on activity and the residuals calculations of ^3H distribution dependent on external controls on activity for b) depth to water, c) summer vs winter rainfall and d) Euclidean distance from the ocean.

3.1 Prediction variances and external drift

The KED grid, produced with 'depth to water' as a covariable, was computed from a fitted Gaussian variogram model with an average semivariance of 0.542 and a planar distance of 89km (Fig.5b). Prediction variance was less localized and formed regional patterns around larger distributions of sample density. High prediction variance regions remained prominent on the east coast and in the upper central Karoo. The KED prediction appeared more gradual in ^3H

distributions with peaks and lows recurring gradually across the country. A similar decrease in average variance and planar distance was observed in KED grids produced with ‘Euclidean distance from ocean’ (Fig.5c) and ‘summer winter rainfall zone’ (Fig.5d). However, the KED grid, produced with ‘summer winter rainfall zone’ as a covariable, had a higher average semivariance of 0.547 and a planar distance of 90km. The KED grid, produced with ‘Euclidean distance from ocean’ as a covariable, had the lowest average semivariance of 0.539 and a planar distance of 89 km.

Furthermore, as all the included environmental co-variables clearly constrain some of the variability of ^{3}H activity in groundwater, the actual spatial structure would be best predicted by including all co-variables in a multivariate ‘universal’ krig or KED. When computed with a residual variogram, with all three co-variables, average semivariance is reduced to 0.531 and the planar distance to 84km (Fig.6). The distribution of prediction variance was more regularly distributed across South Africa, with elevated variance still prominent on the east coast, yet has been substantially lowered with the inclusion of a multivariate approach.

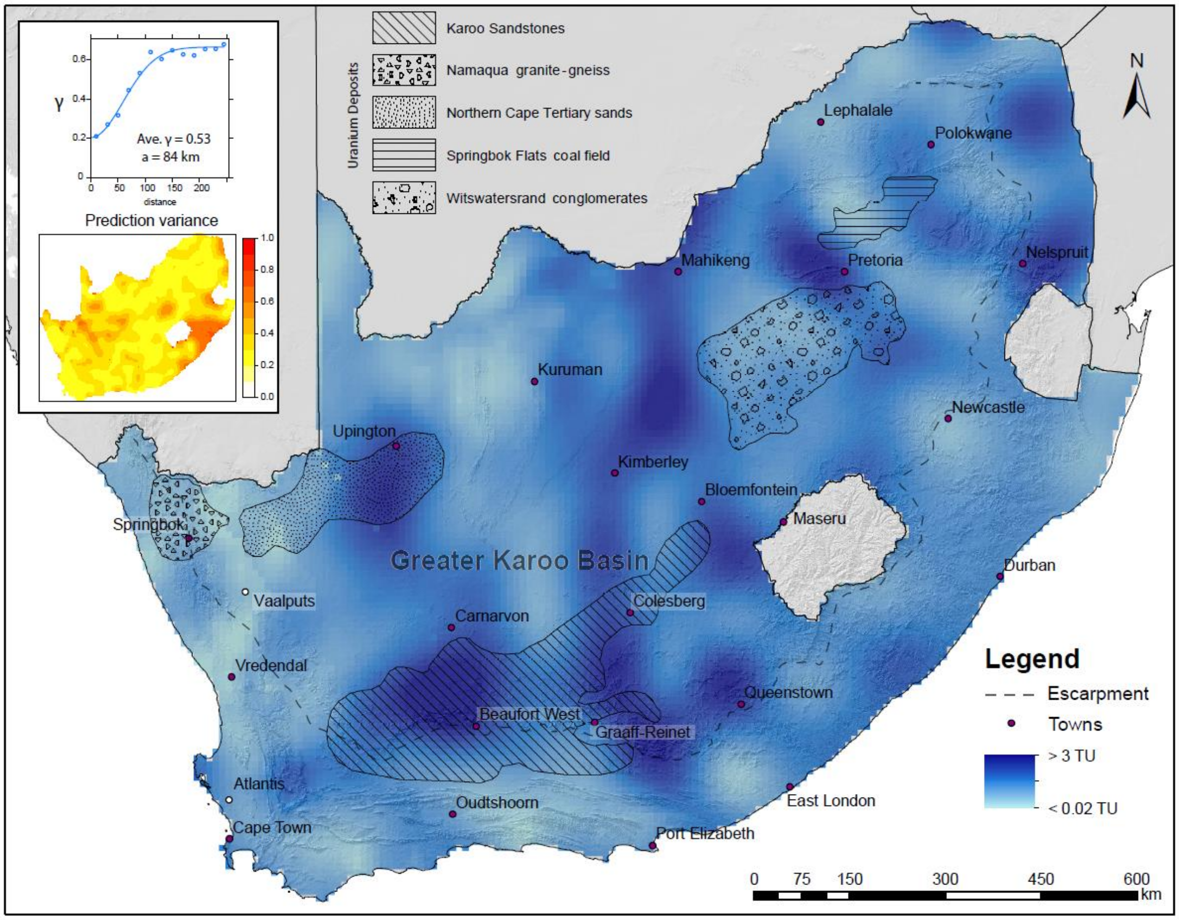

Figure 6 - The predicted distribution of ^{3}H in groundwater by KED with all environmental co-variables. The geostatistical results for variogram fit and prediction variance (top left) and the. uranium deposit extents are overlaid onto the distribution surface as well as the location of the South African escarpment. Locations of interest are included for a radioactive waste disposal site (Vaalputs) and a managed aquifer recharge location (Atlantis).

3.2 Predicted activity of ^{3}H in groundwater

Although the inclusion of environmental co variables greatly improved the prediction variance of ^{3}H, the regional distribution of ^{3}H was still heterogeneous across much of South Africa. The presented KED gridded values of ^{3}H in groundwater, which includes all environmental co-variables, ranged from <0.02 TU to > 3 TU. The highest predicted ^{3}H activities were isolated to regions northwest of the town of Beaufort West and northeast of Kimberly (Fig.6). The northeast of the country near the town of Nelspruit as well as west of Pretoria, generally had elevated ^{3}H activities. The regions of lowest predicted ^{3}H activity occurred on the west and south coasts of South Africa as well as in the northern reaches of the central Karoo. The area around the town of Newcastle also showed low ^{3}H activity in local groundwater. Coastal regions of South Africa had varying degrees of mid to low abundances of ^{3}H and showed partial correlation to South Africa's escarpment. The Karoo basin, which forms the largest aquifer system by extent, generally had higher, albeit variable, ^{3}H activities when compared to the rest of the country.

4 Discussion

Predicting the distribution of ^{3}H activity in groundwater is essential for the assessment of regional recharge processes that effect both groundwater renewability (Gleeson et al., 2016) and modern pollution potential (Jasechko et al., 2017). Yet, regional predictions of groundwater ^{3}H activity can be affected by atmospheric, geographic and hydrogeological processes, including: [1] the variability of tritium in rainfall (van Rooyen et al., 2020a), [2] the decay of tritium in the unsaturated zone during recharge (Harvey et al., 2006; Le Gal La Salle et al., 2001) and, [3] the release of ^{3}H in the subsurface from radioactive deposits (Dresel et al., 2000). The development of KED gridded distributions, that remove the spatial variance of environmental controls, allows for the assessment of: [1] the effective relationship between deeper water tables and ^{3}H activity, [2] the transfer or retention of atmospheric controls of ^{3}H activity in precipitation into the groundwater reservoir and, [3] the correlation of sites or natural features that might distort the atmospheric ^{3}H signal in groundwater.

4.1 Model validation and prediction variance

The performance of the KED model was tested via an out-of-sample verification, where random subsets of the testing data were excluded and then compared to the predicted surface. This was repeated fifteen times, in sample subsets of fifty, to produce a linear relationship of R^2 = 0.554 (Fig.7). The model prediction variance could be greatly improved with better sample distribution and density, as the current distribution is clustered. Similarly, the ^{3}H activities formed a clustered autocorrelation (Moran's I = 0.25). Given the z-score of 20.17, a metric of deviation from the mean, there is a less than 1% likelihood that this clustered pattern could be the result of random chance. An extensive autocorrelation analysis showed that regions of higher sample density were more likely to produce high-low/low-high outliers (Fig.8).

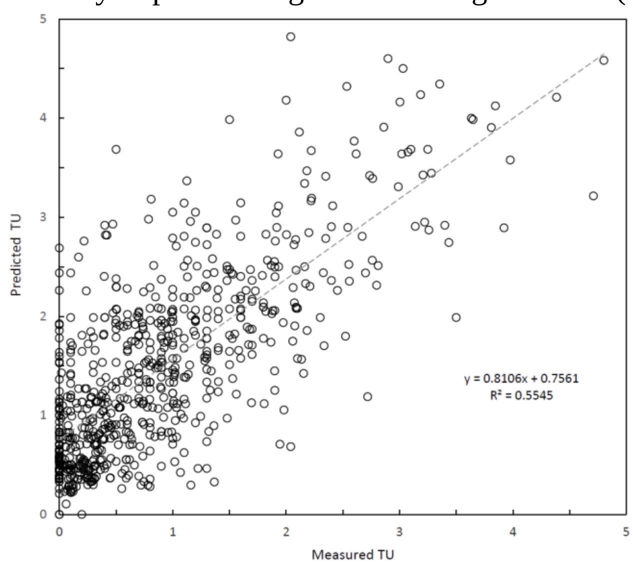

Figure 7 - Measured vs predicted ^{3}H activity in groundwater from the out-of-sample verification method.

Areas of high prediction variance were typically associated with areas of poor sample density, this was evident especially on the east coast of South Africa, as well as the northern central Karoo areas. In order to improve the predictive capabilities of this model, groundwater sampling would need to be done more rigorously in space and time to ‘fill in’ areas of poor sample density and assess the changes in ^{3}H activity over time. The depth to the groundwater table had a significant effect on ^{3}H activity. It would therefore be essential to target regions with deeper groundwater tables to constrain this effect better and in turn calibrate the model for abrupt changes in water table depth. Additionally, groundwater samples lack comprehensive data of borehole screens, leaving this predictive model to assume groundwater in South Africa behaves in one homogenous aquifer unit. Fortunately, this assumption is somewhat mitigated by the decay/flow relationship of tritium in groundwater, where long/slow flow paths will inherently have low ^{3}H activities, negating the need for aquifer separation in most cases. Nonetheless, a separated prediction for alluvial, unconfined and confined systems would improve the applicability for ^{3}H distributions in sustainability/resilience assessments.

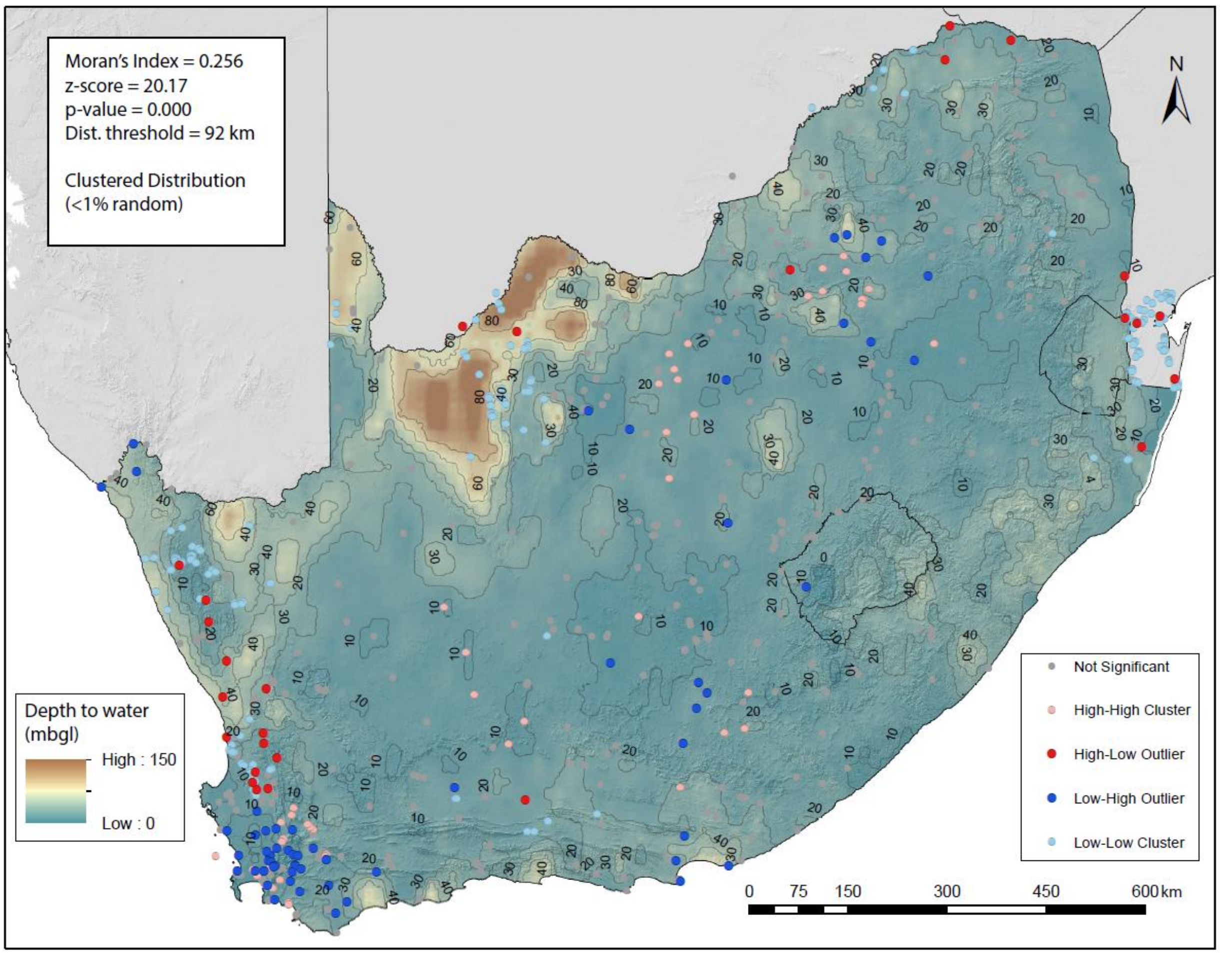

Figure 8 - Autocorrelation results for ^{3}H in groundwater which determines low and high clusters of samples as well as high-low and low-high outliers in the spatial dataset. Included are depth to water contours on the interpolated surface computed for this study.

4.2 Groundwater ^{3}H anomalies

Although the distribution of ^{3}H in groundwater, predicted by KED, was clustered and heterogeneous, the high and low anomalies in the data (Fig.8) correlated well to expected controls on the abundance of ^{3}H. The extensive high ^{3}H anomaly in the central Karoo has a distinct correlation with a large sandstone uranium province (Fig.6) (Kenan and Chirenje, 2016). Although the presence of uranium deposits is not typically associated with elevated groundwater ^{3}H activity, it has been reported that higher uranium concentrations were well correlated with ^{3}H in the Central Valley, California (Jurgens et al., 2010). Uranium deposits in South Africa could potentially produce significant amounts of ^{3}H through the decay, which has high concentrations of uranium in local groundwater (Dondo et al., 2010; Murray et al., 2015; Toens et al., 1998) and thus could elevate the natural signal contributed through recharge. Definitive evidence would need to be collected on ^{3}H production rates in uranium deposits in the region before confirming this contribution is sufficient. A similar phenomena could be attributed to the alluvial uranium-rich deposits south of the town of Upington, where elevated tritium is predicted in a region of low rainfall (Fig.1) and a deeper water table (Fig.8). Conversely, the uranium-rich Witwatersrand conglomerates and the Springbok Flats coalfield, as well as South Africa's only radioactive waste disposal site (Vaalputs), correlate to low tritium anomalies, suggesting that groundwater ^{3}H activity is unaffected by the presence of uranium in these regions (Fig.6). The high anomaly above the town of Queenstown is not correlated to the presence of a uranium deposit, nor a known elevated activity in precipitation, and the region may simply experience higher rates of recharge than surrounding aquifers. Areas of low ^{3}H anomalies generally correlate well to regions of deeper water tables, this is especially evident on the west coast, northern Karoo and north of the city of Pretoria.

4.3 ^{3}H and modern groundwater distributions

Modern recharge typically shares a similar ^{3}H activity to local precipitation available for recharge. Where groundwater ^{3}H anomalies cannot be explained by environmental factors that cause drift from recharge activities, active recharge is proportional to ^{3}H activity (Gleeson et al., 2016). The distribution of tritium in South African groundwater, unaffected by non-atmospheric ^{3}H, is somewhat consistent with the expected activity of ^{3}H in precipitation (van Rooyen et al., 2020a), where coastal regions have lower activity than inland regions (Fig.6). The effect of ocean water dilution in rainfall is not directly correlated with the distance from ocean of measured groundwater samples ($R^2 = 0.03$). However, coastal regions (<100 km from the ocean) generally have lower average ^{3}H activities that are not likely a result of less active recharge, as productive coastal aquifers are prevalent in South Africa (Pietersen et al., 2010). This would suggest that the effect of ocean dilution is experienced within a particular threshold of distance from the coast, potentially the South African escarpment, but not further inland where terrestrial processes dominate (Fig.6).

It is not clear what effect groundwater abstraction is on ^{3}H activity, yet boreholes that are pumped excessively could induce the mixing of younger waters into deeper older systems, thus increasing ^{3}H activity (Visser et al., 2016). Anthropogenic influences, particularly dewatering of aquifers, on groundwater mixing could result in the overestimation of active recharge areas where groundwater use is particularly high. Conversely, managed aquifer recharge (MAR) programs would introduce ^{3}H faster than natural recharge processes, making measured ^{3}H activities non-representative. A known region of MAR, near Atlantis (Fig.6) is not predicted to have elevated ^{3}H activity and could be introducing ^{3}H at a localized scale too small for the resolution of this study.

Elevated ^{3}H activity within large aquifers in South Africa indicates that these groundwater resources are being actively recharged by modern precipitation. Research suggests that much of South Africa will experience less frequent, but higher intensity, rainfall due to climate change (Schulze et al., 2010; Tadross et al., 2011). As a consequence, these aquifers are particularly vulnerable to climate change, where changes in regional rainfall volumes and intensity will effect recharge (Taylor et al., 2013). Furthermore, areas of active recharge have a greater potential for contaminants to be transported into an aquifer. Regions were groundwater is abundant and aquifer yields are high, yet ^{3}H activity is low in relation to local rainfall, represent regions where recharge is less active and fossil groundwater is prevalent. Although older groundwater may have a lower sustainable yield, it is less likely to be immediately affected by climate change and may be more resilient to abrupt changes to the hydrological cycle.

4.4 Current and future context of ^{3}H distributions

The distribution of ^{3}H in groundwater has been successfully used to predict modern groundwater distributions (Gleeson et al., 2016), deep groundwater contamination (Jasechko et al., 2017), groundwater contribution to streamflow (Morgenstern et al., 2010), pollutant transport from landfills (Robinson and Gronow, 1996), nuclear fall-out (Matsumoto et al., 2013) and groundwater vulnerability (van Rooyen et al., 2020b). Yet, the availability of ^{3}H activity distributions, as an interpolated surface, is uncommon or non-existent, as studies do not typically measure ^{3}H over large spatial extents with regular distributions. This may be a result of researches believing the applicability of ^{3}H in hydrological studies is dissipating with the attenuation of bomb peak activities (Rahn et al., 2017). However, with the progression of analytical techniques, the assessment of background levels of tritium presents new potential applications of ^{3}H in hydrology and related fields of study. It is postulated in this study that the presence of radioactive deposits (i.e. uranium) may have a substantial affect on^{3}H activity, suggesting ^{3}H could have applications in exploration. Nonetheless, more robust interpretations of the above uses for ^{3}H distributions could be made with regular monitoring of well distributed samples locations, as were in California by Visser et al., (2016). A similar approach was undertaken in Kern et al., (2020), where temporal records of precipitation from multiple stations in the Adriatic-Pannonian region were used to build isoscapes of ^{3}H in precipitation. The monitoring of environmental ^{3}H at such a resolution that isoscapes can be compared over time would require an improvement in local analytical capabilities in southern Africa.

5 Conclusions

Analysis of 722 data points across South Africa and southern Mozambique found that the spatial distribution of ^{3}H activities in groundwater was relatively heterogeneous. Yet, geostatistical analysis found that significant spatial structure can be attributed to environmental controls on activity other than subsurface decay. When excluded as external drift in universal kriging operations, environmental controls improve the average prediction semivariance by 0.03. Significant high ^{3}H anomalies in the predicted distribution in groundwater could attributed to the presence of uranium rich deposits in the Karoo Basin sandstones and northern Karoo alluvial deposits, yet more evidence would need to be collected to propose this definitively. Notable areas of less active groundwater recharge occurred on the west coast of South Africa as well as the central and northern Karoo. Regions of more active recharge are noted in the north eastern regions of South Africa as well the western borders of Lesotho. Regions of active recharge are more vulnerable to disruptions to the hydrological cycle as a result of climate change as well as the potential infiltration of contaminants into the groundwater system. Conversely, groundwater that is less actively recharge may be more resilient to climate change, yet represents a potentially non-renewable resource for abstraction. The distribution of ^{3}H in groundwater surface developed in this study has potential applications in modern groundwater distribution, groundwater vulnerability and radioactive deposit investigations. Applications which are pertinent to the development of sustainable groundwater management strategies and hydrological resilience assessments.

Acknowledgments

We thank the Water Research Commission South Africa for initial funding support and the iPhakade program and National Research Foundation South Africa for bursary support. This work is also based on research supported in part by the National Research Foundation of South Africa (Grant number: 118594) and was partly supported by the European Union and the State of Hungary, co-financed by the European Regional Development Fund in the project of GINOP-2.3.2-15-2016-00009 'ICER'. The authors would like to acknowledge the assistance of the University of Utah's ITCE SPATIAL program for providing the training necessary to construct the model presented in this paper. This publication forms part of the output of the Biogeochemistry Research Infrastructure Platform (BIOGRIP) of the Department of Science and Innovation of South Africa. This contribution has an iPhakade publication number of 257.

References

Basson, M.S., Van Niekerk, P.H., Van Rooyen, J.A., 1997. Overview of water resources availability and utilisation in South Africa. Department of Water Affairs and Forestry.

Bennetts, D.A., Webb, J.A., Stone, D.J.M., Hill, D.M., 2006. Understanding the salinisation process for groundwater in an area of south-eastern Australia, using hydrochemical and isotopic evidence. J. Hydrol. 323, 178–192. https://doi.org/10.1016/j.jhydrol.2005.08.023

Böhlke, J.K., 2002. Groundwater recharge and agricultural contamination. Hydrogeol. J. 10, 153–179. https://doi.org/10.1007/s10040-001-0183-3

Böhlke, J.K., Denver, J.M., 1995. Combined use of groundwater dating, chemical, and isotopic analyses to resolve the history and fate of nitrate contamination in two agricultural watersheds, Atlantic coastal plain, Maryland. Water Resour. Res. 31, 2319–2339.

Chilès, J.-P., 2012. The Generalized Variogram 33.

Cobbing, J.E., Hobbs, P.J., Meyer, R., Davies, J., 2008. A critical overview of transboundary aquifers shared by South Africa. Hydrogeol. J. 16, 1207–1214. https://doi.org/10.1007/s10040-008-0285-2

Cuthbert, M.O., Gleeson, T., Moosdorf, N., Befus, K.M., Schneider, A., Hartmann, J., Lehner, B., 2019. Global patterns and dynamics of climate–groundwater interactions. Nat. Clim. Chang. 9, 137–141. https://doi.org/10.1038/s41558-018-0386-4

Díaz-Cruz, M.S., Barceló, D., 2008. Trace organic chemicals contamination in ground water recharge. Chemosphere 72, 333–342. https://doi.org/10.1016/j.chemosphere.2008.02.031

Dondo, C., Woodford, A.C., Murray, R., Nhleko, L.O., Gqiba, D., Chevallier, L., 2010. Flow conceptualisation, recharge and storativity determination in karoo aquifers, with special emphasis on Mzimvubu Keiskamma and Mvoti-Umzimkulu water management areas in the Eastern Cape and Kwazulu-Natal provinces of South Africa. WRC Rep.

Dresel, P.E., Williams, B.A., Evans, J.C., Smith, R.M., Thompson, C.J., Hulstrom, L.C., Dresel, P.E., Williams, B.A., Evans, J.C., Smith, R.M., Thompson, C.J., Hulstrom, L.C., 2000. Evaluation of Elevated Tritium Levels in Groundwater Downgradient from the 618-11 Burial Ground Phase I Investigation.

DWAF, 2004. Overview of the South African Water Sector. Natl. water Resour. Strateg. 1, 1–35.

Ferguson, G., Gleeson, T., 2012. Vulnerability of coastal aquifers to groundwater use and climate change. Nat. Clim. Chang. 2, 342–345. https://doi.org/10.1038/nclimate1413

Gillon, M., Barbecot, F., Gibert, E., Corcho Alvarado, J.A., Marlin, C., Massault, M., 2009. Open to closed system transition traced through the TDIC isotopic signature at the aquifer recharge stage, implications for groundwater 14C dating. Geochim. Cosmochim. Acta 73, 6488–6501. https://doi.org/10.1016/j.gca.2009.07.032

Gleeson, T., Befus, K.M., Jasechko, S., Luijendijk, E., Cardenas, M.B., 2016. The global volume and distribution of modern groundwater. Nat. Geosci. 9, 161–164. https://doi.org/10.1038/ngeo2590

Gleeson, T., Befus, K.M., Jasechko, S., Luijendijk, E., Cardenas, M.B., 2015. The global volume and distribution of modern groundwater. Nat. Geosci. Advance on, 1–15. https://doi.org/10.1038/ngeo2590

Hagedorn, B., Clarke, N., Ruane, M., Faulkner, K., 2018. Assessing aquifer vulnerability from lumped parameter modeling of modern water proportions in groundwater mixtures: Application to California’s South Coast Range. Sci. Total Environ. 624, 1550–1560. https://doi.org/10.1016/j.scitotenv.2017.12.115

Harms, P.A., Visser, A., Moran, J.E., Esser, B.K., 2016. Distribution of tritium in precipitation and surface water in California. J. Hydrol. 534, 63–72.

Harvey, J.W., Newlin, J.T., Krupa, S.L., 2006. Modeling decadal timescale interactions between surface water and ground water in the central Everglades, Florida, USA. J. Hydrol. 320, 400–420. https://doi.org/10.1016/J.JHYDROL.2005.07.024

Hughes, C.E., Cendón, D.I., Harrison, J.J., Hankin, S.I., Johansen, M.P., Payne, T.E., Vine, M., Collins, R.N., Hoffmann, E.L., Loosz, T., 2011. Movement of a tritium plume in shallow groundwater at a legacy low-level radioactive waste disposal site in eastern Australia. J. Environ. Radioact. 102, 943–952. https://doi.org/10.1016/j.jenvrad.2010.05.009

Jasechko, S., Perrone, D., Befus, K.M., Bayani Cardenas, M., Ferguson, G., Gleeson, T., Luijendijk, E., McDonnell, J.J., Taylor, R.G., Wada, Y., Kirchner, J.W., 2017. Global aquifers dominated by fossil groundwaters but wells vulnerable to modern contamination. Nat. Geosci. 10, 425–429. https://doi.org/10.1038/ngeo2943

Jurgens, B.C., Fram, M.S., Belitz, K., Burow, K.R., Landon, M.K., 2010. Effects of Groundwater Development on Uranium: Central Valley, California, USA. Ground Water 48, 913–928. https://doi.org/10.1111/j.1745-6584.2009.00635.x

Kenan, A.O., Chirenje, E., 2016. Uranium in South Africa: Exploration and Supply Capacity. Nat. Resour. Conserv. 4, 25–33. https://doi.org/10.13189/nrc.2016.040201

Kern, Z., Erdélyi, D., Vreča, P., Krajcar Bronić, I., Fórizs, I., Kanduč, T., Štrok, M., Palcsu, L., Süveges, M., Czuppon, G., Kohán, B., Gábor Hatvani, I., 2020. Isoscape of amount-weighted annual mean precipitation tritium (³H) activity from 1976 to 2017 for the Adriatic–Pannonian region – AP³H_v1 database. Earth Syst. Sci. Data 12, 2061–2073. https://doi.org/10.5194/essd-12-2061-2020

Le Gal La Salle, C., Marlin, C., Leduc, C., Taupin, J.D., Massault, M., Favreau, G., 2001. Renewal rate estimation of groundwater based on radioactive tracers (3H, 14C) in an unconfined aquifer in a semi-arid area, Iullemeden basin, Niger. J. Hydrol. 254, 145–156. https://doi.org/10.1016/S0022-1694(01)00491-7

Li, Z., Jasechko, S., Si, B., 2019. Uncertainties in tritium mass balance models for groundwater recharge estimation. J. Hydrol. 571, 150–158. https://doi.org/10.1016/j.jhydrol.2019.01.030

Lucas, L.L., Unterweger, M.P., 2000. Comprehensive Review and Critical Evaluation of the Half-Life of Tritium. J. Res. Natl. Inst. Stand. Technol. 105, 541–549. https://doi.org/10.6028/jres.105.043

MacMahon, D., 2006. Half-life evaluations for 3H, 90Sr, and 90Y. Appl. Radiat. Isot. 64, 1417–1419. https://doi.org/10.1016/j.apradiso.2006.02.072

Mao, F., Clark, J., Karpouzoglou, T., Dewulf, A., Buytaert, W., Hannah, D., 2017. HESS Opinions: A conceptual framework for assessing socio-hydrological resilience under change. Hydrol. Earth Syst. Sci. 21, 3655–3670. https://doi.org/10.5194/hess-21-3655-2017

Matheron, G., 1965. Les variables régionalisées et leur estimation: une application de la théorie des fonctions aléatoires aux sciences de la nature. Masson et CIE.

Matsumoto, T., Maruoka, T., Shimoda, G., Obata, H., Kagi, H., Suzuki, K., Yamamoto, K., Mitsuguchi, T., Hagino, K., Tomioka, N., Sambandam, C., Brummer, D., Klaus, P.M., Aggarwal, P., 2013. Tritium in Japanese precipitation following the March 2011 Fukushima Daiichi Nuclear Plant accident. Sci. Total Environ. 445–446, 365–370. https://doi.org/10.1016/j.scitotenv.2012.12.069

Meixner, T., Manning, A.H., Stonestrom, D.A., Allen, D.M., Ajami, H., Blasch, K.W., Brookfield, A.E., Castro, C.L., Clark, J.F., Gochis, D.J., Flint, A.L., Neff, K.L., Niraula, R., Rodell, M., Scanlon, B.R., Singha, K., Walvoord, M.A., 2016. Implications of projected climate change for groundwater recharge in the western United States. J. Hydrol. 534, 124–138. https://doi.org/10.1016/j.jhydrol.2015.12.027

Morgenstern, U., Stewart, M.K., Stenger, R., 2010. Dating of streamwater using tritium in a post nuclear bomb pulse world: Continuous variation of mean transit time with streamflow. Hydrol. Earth Syst. Sci. 14, 2289–2301. https://doi.org/10.5194/hess-14-2289-2010

Murray, R., Swana, K., Miller, J., Talma, S., Tredoux, G., Vengosh, A., Darrah, T., 2015. The Use of Chemistry, Isotopes and Gases as Indicators of Deeper Circulating Groundwater in the Main Karoo Basin: Report to the Water Research Commission. Water Research Commission.

Niang, I., Ruppel, O.C., Abdrabo, M.A., Essel, A., Lennard, C., Padgham, J., Urquhart, P., 2014. Africa Climate Change 2014: Impacts, Adaptation, and Vulnerability. Part B: Regional Aspects. Contribution of Working Group II to the Fifth Assessment Report of the Intergovernmental Panel on Climate Change ed VR Barros et al.

Palcsu, L., Kompár, L., Deák, J., Szucs, P., Papp, L., 2017. Estimation of the natural groundwater recharge using tritium-peak and tritium/helium-3 dating techniques in Hungary. Geochem. J. 51, 439–448. https://doi.org/10.2343/geochemj.2.0488

Palcsu, L., Major, Z., Köllő, Z., Papp, L., 2010. Using an ultrapure 4He spike in tritium measurements of environmental water samples by the 3He-ingrowth method. Rapid Commun. Mass Spectrom. An Int. J. Devoted to Rapid Dissem. Up-to-the-Minute Res. Mass Spectrom. 24, 698–704.

Papp, L., Palcsu, L., Major, Z., Rinyu, L., Tóth, I., 2012. A mass spectrometric line for tritium analysis of water and noble gas measurements from different water amounts in the range of microlitres and millilitres noble gas measurements from different water amounts in the. Isot. envrionmental 6016. https://doi.org/10.1080/10256016.2012.679935

Pietersen, K., Kellgren, N., Roos, M., De Vries, P., 2010. Explanatory Brochure for the South African Development Community (SADC) Hydrogeological Map & Atlas. Explan. Broch. South African Dev. Community 1–51.

Plastino, W., Chereji, I., Cuna, S., Kaihola, L., De Felice, P., Lupsa, N., Balas, G., Mirel, V., Berdea, P., Baciu, C., 2007. Tritium in water electrolytic enrichment and liquid scintillation counting. Radiat. Meas. 42, 68–73. https://doi.org/10.1016/j.radmeas.2006.07.010

Ploner, A., 1999. The use of the variogram cloud in geostatistical modelling. Environmetrics 10, 413–437. https://doi.org/10.1002/(sici)1099-095x(199907/08)10:4<413::aid-env365>3.0.co;2-u

Rahn, P.H., Detwiler, A.G., Davis, A.D., 2017. Tritium in groundwater in the Black Hills of South Dakota. Environ. Earth Sci. 76, 1–11. https://doi.org/10.1007/s12665-017-7082-y

Robinson, H.D., Gronow, J.R., 1996. Tritium levels in leachates and condensates from domestic wastes in landfill sites. Water Environ. J. 10, 391–398. https://doi.org/10.1111/j.1747-6593.1996.tb00070.x

Roffe, S.J., Fitchett, J.M., Curtis, C.J., 2019. Classifying and mapping rainfall seasonality in South Africa: a review. South African Geogr. J. 101, 158–174. https://doi.org/10.1080/03736245.2019.1573151

Rossiter, D.G., Eda, N., 2019. An introduction to (geo) statistics with R.

Samborska, K., Rózkowski, A., Małoszewski, P., 2013. Estimation of groundwater residence time using environmental radioisotopes (14C,T) in carbonate aquifers, southern Poland. Isotopes Environ. Health Stud. 49, 73–97. https://doi.org/10.1080/10256016.2012.677041

Schlosser, P., Stute, M., Sonntag, C., Otto Münnich, K., 1989. Tritiogenic 3He in shallow groundwater. Earth Planet. Sci. Lett. 94, 245–256. https://doi.org/10.1016/0012-821X(89)90144-1

Schoups, G., Hopmans, J.W., Young, C.A., Vrugt, J.A., Wallender, W.W., Tanji, K.K., Panday, S., 2005. Sustainability of irrigated agriculture in the San Joaquin Valley, California. Proc. Natl. Acad. Sci. 102, 15352–15356. https://doi.org/10.1073/pnas.0507723102

Schulze, R., Kunz, R., Knoesen, D., 2010. Atlas of climate change and water resources in South Africa. Water Res. Comm. Pretoria, Pretoria.

Schulze, R.E., Lynch, S.D., Maharaj, M., 2006. Annual Precipitation. South African Atlas Climatol. Agrohydrology. Water Res. Comm. Pretoria, RSA, WRC Rep. 489/1/06, Section 6.2.

Stewart, M.K., 2012. A 40-year record of carbon-14 and tritium in the Christchurch groundwater system, New Zealand: Dating of young samples with carbon-14. J. Hydrol. 430–431, 50–68. https://doi.org/10.1016/j.jhydrol.2012.01.046

Tadross, M., Davis, C., Engelbrecht, F., Joubert, A., Archer, E.R.M., 2011. Regional scenarios of future climate change over southern Africa. CSIR.

Taylor, R.G., Todd, M.C., Kongola, L., Maurice, L., Nahozya, E., Sanga, H., Macdonald, A.M., 2013. Evidence of the dependence of groundwater resources on extreme rainfall in East Africa. Nat. Clim. Chang. 3, 374–378. https://doi.org/10.1038/nclimate1731

Toens, P.D., Standler, W., Wullschleger, N.J., 1998. The association of groundwater chemistry and geology with atypical lymphocytes (as a biological indicator) in the Pofadder area, North Western Cape, South Africa 64.

van Rooyen, J.D., Palcsu, L., Visser, A., Vennemann, T.W., Miller, J.A., 2020a. Spatial and temporal variability of tritium in precipitation in South Africa and it’s bearing on hydrological studies. J. Environ. Radioact. 106354. https://doi.org/10.1016/j.jenvrad.2020.106354

van Rooyen, J.D., Watson, A.P., Miller, J.A., 2020b. Combining quantity and quality controls to determine groundwater vulnerability to depletion and deterioration throughout South Africa. Environ. Earth Sci. 79. https://doi.org/10.1007/s12665-020-08998-1

Vengosh, A., Gill, J., Davisson, M.L., Hudson, G.B., 2002. A Multi-lsotope .(B , Sr , O , H , C) and Age Dating (3H-3He , ~ 4C) Study of Ground Water from Salinas Valley California : Hydrochemistry , Dynamics , and Contamination Processes. Water Resour. Res. 38, 9 1-17. https://doi.org/10.1029/2001WR000517

Villholth, K.G., Tøttrup, C., Stendel, M., Maherry, A., 2013. Integrated mapping of groundwater drought risk in the Southern African Development Community (SADC) region. Hydrogeol. J. 21, 863–885. https://doi.org/10.1007/s10040-013-0968-1

Visser, A., Moran, J.E., Hillegonds, D., Singleton, M.J., Kulongoski, J.T., Belitz, K., Esser, B.K., 2016. Geostatistical analysis of tritium, groundwater age and other noble gas derived parameters in California. Water Res. 91, 314–330. https://doi.org/10.1016/j.watres.2016.01.004

Visser, A., Thaw, M., Esser, B., 2018. Analysis of air mass trajectories to explain observed variability of tritium in precipitation at the Southern Sierra Critical Zone Observatory, California, USA. J. Environ. Radioact. 181, 42–51. https://doi.org/10.1016/j.jenvrad.2017.10.008

Wada, Y., Van Beek, L.P.H., Van Kempen, C.M., Reckman, J.W.T.M., Vasak, S., Bierkens, M.F.P., 2010. Global depletion of groundwater resources. Geophys. Res. Lett. 37, 1–5. https://doi.org/10.1029/2010GL044571

West, J.B., Bowen, G.J., Dawson, T.E., Tu, K.P., 2009. Isoscapes: understanding movement, pattern, and process on Earth through isotope mapping. Springer.

Zhang, L., Dawes, W.R., Walker, G.R., 2001. Response of mean annual evapotranspiration to vegetation changes at catchment scale. Water Resour. Res. 37, 701–708.

Zuber, A., Witczak, S., Rózański, K., Śliwka, I., Opoka, M., Mochalski, P., Kuc, T., Karlikowska, J., Kania, J., Jackowicz-Korczyński, M., Duliński, M., 2005. Groundwater dating with 3H and SF6 in relation to mixing patterns, transport modelling and hydrochemistry. Hydrol. Process. 19, 2247–2275. https://doi.org/10.1002/hyp.5669